

8

Magnetic Levitation

Clement Lorin¹, Richard J. A. Hill² and Alain Mailfert³

¹Mechanical Engineering Department, University of Houston,
Houston, TX, USA

²School of Physics and Astronomy, University of Nottingham,
Nottingham, UK

³Laboratoire Géoresources, CNRS-Université de Lorraine,
Nancy, France

8.1 Introduction

To compensate gravity magnetically, one generates at all points within an object—at the molecular scale—magnetic forces that counterbalance the force of gravity. This form of magnetic levitation, distinct from levitation of a ferromagnet or superconductor, or flotation, exploits the fact that a diamagnetic or paramagnetic medium is subjected to a magnetic body force in a non-uniform magnetic field. Suitable magnetic field sources for levitation include windings carrying continuous currents and in some cases permanent magnets. The first simulations of space conditions by levitation in fluids or biological systems were reported using water-cooled or superconducting magnets [1–4]. Magnetic compensation of gravity has many advantages compared to other ways to access weightlessness, such as unlimited experimentation time, ground-based experiments, and easily adjustable level of simulated gravity. It is the only way to directly compensate gravity at the molecular level, on the ground. Partial gravity compensation allows simulation of the gravity on Moon or Mars [5]. Here, we discuss the accuracy with which one can compensate gravity using magnetic levitation, for fluids and for biology.

8.2 Static Magnetic Forces in a Continuous Medium

8.2.1 Magnetic Forces and Gravity, Magneto-Gravitational Potential

Windings carrying electrical currents with a volume density \mathbf{J} (A m^{-2}) or magnetized magnetic media [magnetization density \mathbf{M} (A m^{-1})] generate a magnetic field of excitation \mathbf{H} (A m^{-1}). Experimentally, one measures the magnetic flux density \mathbf{B} (T or Wb m^{-2}). In free space, $\mathbf{B} = \mu_0 \mathbf{H}$ where $\mu_0 = 4\pi \times 10^{-7} \text{ H m}^{-1}$ is the vacuum permeability. The relations between these quantities are, in stationary (time-independent) conditions, as follows:

$$\mathbf{curl}(\mathbf{H}) = \mathbf{J}; \quad \text{div}(\mathbf{B}) = 0 \quad (8.1)$$

in a current-free domain:

$$\mathbf{curl}(\mathbf{H}) = \mathbf{0} \quad (8.2)$$

A magnetic field \mathbf{H} applied to any homogeneous material (solid or fluid) produces a magnetization density:

$$\mathbf{M}(\mathbf{H}) = \chi \mathbf{H}. \quad (8.3)$$

The dimensionless magnetic susceptibility χ can be positive (paramagnetism) or negative (diamagnetism). We will take into account non-hysteretic media with χ considered as a constant when the magnetic field varies. That is neither ferromagnetic media nor colloidal suspensions of particles, namely ferrofluids.

In these media, the flux density is as follows: $\mathbf{B} = \mu_0 (\mathbf{H} + \mathbf{M}) = \mu_0 (1 + \chi) \mathbf{H}$, where $\mu_0(1 + \chi)$ is the medium magnetic permeability.

The above relations give unique solutions for \mathbf{H} and \mathbf{B} , given distributions for \mathbf{J} and \mathbf{M} . However, the “designers” of a levitation magnet have to solve the “inverse problem”: Which configurations of \mathbf{J} and \mathbf{M} can create given distributions of \mathbf{H} and \mathbf{B} inside a finite 3D domain? This problem has numerous possible solutions.

A magnetic energy is associated with the magnetization that appears in materials. If the field \mathbf{H} varies spatially, the magnetic energy varies spatially, too. A magnetic material is thus subjected to a volume force that can be written as follows:

$$\mathbf{f}_m = \frac{\mu_0}{2} \chi \mathbf{grad}(\mathbf{H}^2)$$

In materials that are considered for magnetic levitation, $|\chi| \ll 1$, that is $\mu_0(1 + \chi) \sim \mu_0$. Therefore, the magnetic volume force can likewise be expressed as follows:

$$\mathbf{f}_m = \frac{1}{2\mu_0} \chi \mathbf{G} \quad (8.4)$$

Table 8.1 Order of magnitude of some fluid features for magnetic compensation of gravity

Fluid ($P = 1$ bar, $g = 9.81$ m s $^{-2}$)	O ₂ (90 K)	H ₂ (20 K)	H ₂ O (293 K)	He (4.2 K)
Magnetic susceptibility (10^{-6})	+3,500	-1.8	-9.0	-0.74
Density (kg m $^{-3}$)	1,140	71	998	125
G_1 (T 2 m $^{-1}$)	+8	-990	-2,720	-4,140

where $\mathbf{G} = \mathbf{grad}(\mathbf{B}^2)$. The principle of magnetic gravity compensation is based on relation (8.4). The magnetic force must be opposite to the force applied by gravity \mathbf{g} (m s $^{-2}$): $\mathbf{f}_G = \rho\mathbf{g}$.

Therefore, the condition of magnetic compensation at any point within a medium of susceptibility χ and density ρ is

$$\mathbf{grad}(\mathbf{B}^2) = -2\mu_0 \frac{\rho}{\chi} \mathbf{g} = \mathbf{G}_1 \quad (8.5)$$

where (χ/ρ) (m 3 kg $^{-1}$) is the mass susceptibility. It is also useful to consider the total resulting potential energy Σ_L (J m $^{-3}$), named magneto-gravitational potential (MG potential), at a given height z (m) [3].

$$\Sigma_L = \frac{\chi B^2}{2\mu_0} - \rho g z$$

From relation (8.5), Table 8.1 gives some algebraic values of \mathbf{G}_1 needed to compensate gravity for various fluids commonly used in aerospace engineering.

8.2.2 Magnetic Compensation Homogeneity

There is a fundamental constraint for magnetic compensation of gravity. A given \mathbf{B} distribution leads to a unique force distribution, but an arbitrary force distribution cannot be obtained. Indeed, in a 3D domain, small with respect to the size of Earth, the terrestrial acceleration is independent of position, that is \mathbf{G} should be uniform to satisfy (8.5). Since magnetic flux density \mathbf{B} obeys (8.1) and (8.2), \mathbf{G} cannot be simultaneously nonzero and uniform in the whole 3D domain [6]; it follows that it is impossible to obtain perfect compensation of gravity at every point in space! However, there exist magnetic field distributions where compensation is perfect in several points, or along a vertical segment line, or on a horizontal plane. It follows from the previous theorem that it is impossible to magnetically compensate any force field with a zero divergence. But it has been shown theoretically [7] that for

diamagnetic materials, gravity can be compensated exactly, in the whole 3D domain with translational invariance, by combination of both magnetic and centrifugal forces Ω (note that $\text{div}(\Omega) \neq 0$). No experimental verification of this last property has been carried out yet. In the absence of Ω , we define a (dimensionless) inhomogeneity vector ε which represents the relative error between the \mathbf{G} produced by the magnet and that required for perfect gravity compensation \mathbf{G}_1 ,

$$\varepsilon = \frac{\mathbf{G} - \mathbf{G}_1}{\overline{G_1}}$$

Here, $\overline{G_1}$ is the algebraic value of \mathbf{G}_1 ; that is, $\overline{G_1}$ is positive for paramagnetic materials and negative for diamagnetic ones ($\overline{G_1}$ is written G_1 up to the end of the section). The quality of the compensation can be directly visualized by mapping the vector field ε . Indeed, the latter represents the residual acceleration $\Gamma = g\varepsilon$, which can be interpreted as an effective gravitational field Γ . In order to use magnetic compensation method, one first has to define what approximation to the exact compensation is needed inside the working zone.

8.3 Axisymmetric Levitation Facilities

Levitation devices are usually made of axisymmetric windings. An analysis is first developed for a single vertical-axis solenoid and then extended to more complex systems.

8.3.1 Single Solenoids

Figure 8.1 shows the magnetic compensation obtained using a solenoid current I high enough to for the magnetic force to balance gravity at two points, one stable (+) and one unstable (\times), on the solenoid axis. In the right-hand panel, I is larger than in the left, showing that the axial location of the points (+, \times), the shape of the MG equipotentials (MGE), and the resulting acceleration ε depend on I .

Using Taylor polynomial approximations of the relevant quantities, one can establish relations between the components of the inhomogeneity vector (ε_r and ε_z in cylindrical coordinates) at a point a distance R from the perfect magnetic compensation point (+) and the norm B of the magnetic flux density at this point for a given fluid (G_1 constant). The first-order approximation in axisymmetric levitation facilities such as the above solenoid leads to

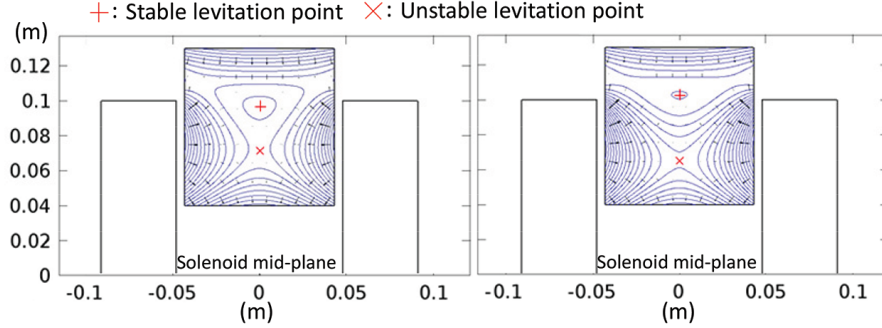


Figure 8.1 MGE (blue curves) and inhomogeneity ε (black arrows) in an arbitrary volume surrounding both points of perfect compensation along the solenoid axis, for two different currents. Dimensions are those of solenoid HyLDe used at the French Atomic Energy Commission (CEA Grenoble) for LH2. The stable point (plus symbol) is at the bottom of a local potential well, and the unstable point (multiplication symbol) is a saddle point in the potential.

$$B = \frac{1}{2} \left[\frac{3|G_1|R}{2\varepsilon_r + \varepsilon_z} \right]^{\frac{1}{2}}$$

It is worth noticing that R/ε varies as the square of the magnetic flux density for a given fluid. Therefore, high magnetic field facilities are used to reach better magnetic compensation or larger levitated volumes. This expression shows that the levitation in a 1-mm-radius sphere, with a maximal isotropic homogeneity of 99 %, that is $\varepsilon_r = \varepsilon_z = 1$ %, requires a magnetic flux density of 5.0 T for hydrogen ($G_1 = -990 \text{ T}^2 \text{ m}^{-1}$) and 8.3 T for water ($G_1 = -2,740 \text{ T}^2 \text{ m}^{-1}$). But the shape of isohomogeneity zones near the compensation point is not necessarily spherical: They may be ellipsoidal, as it will be shown below. A spherical harmonic analysis of the magnetic field allows one to determine analytically the resulting acceleration around the perfect stable compensation point; the results are given in Figure 8.2, encapsulating the diamagnetic compensation performance of the superconducting single solenoid HyLDe. The C_n coefficient (C_1 , C_2 , or C_3 in Figure 8.2) is the n th spherical harmonic coefficient of the magnetic scalar potential W : $W_n = C_n r^n P_n(\cos \theta)$ where W_n is the n th harmonic of the magnetic scalar potential inside the magnetic field sources, r is the radius, θ is the polar angle of the spherical coordinate system, and P_n is the n th-degree Legendre polynomial. The magnetic field derives from this potential: $\mathbf{H} = \mathbf{grad}(-W)$. The C_n coefficients vary depending on the origin of the coordinate system along the axis as shown in Figure 8.2.

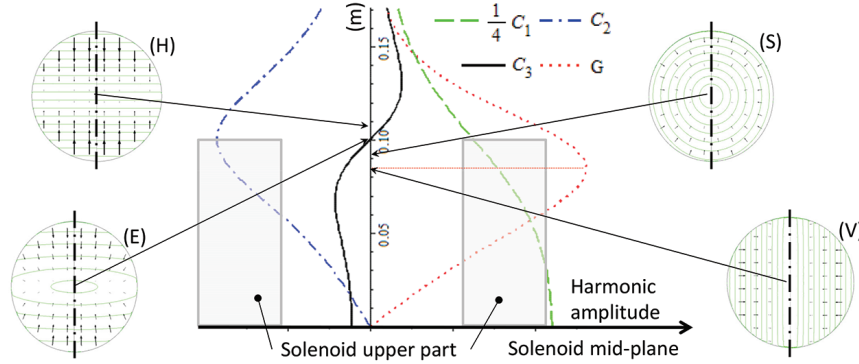


Figure 8.2 Variations of first three spherical harmonics (C_1 , C_2 , C_3) of the scalar potential W of the field, along the *upper part* of the axis of the solenoid (HyLDe) at a given current. The *red dotted line* is the amplitude of the vector \mathbf{G} (proportional to C_1 times C_2). On the axis are located the first levitation point (V) and three other specific levitation points (S, E, H). The levitations occur, respectively, at $z_V = 0.085$ m, $z_S = 0.092$ m, $z_E = 0.101$ m, and $z_H = 0.113$ m at different current values I_V , $I_S/I_V = 1.012$, $I_E/I_V = 1.060$, and $I_H/I_V = 1.111$. The theoretical shapes of the MG potential wells surrounding the levitation points as well as the resulting acceleration (*black arrows*) are plotted.

The red dotted line gives, along the solenoid axis, the vertical component of the volume force f_m , which is proportional to the square of the solenoid current, I . At a value $I = I_V$ of the current, the first levitation point is reached for liquid hydrogen (LH2), at a point V on the axis. For $I > I_V$, two levitation points exist along the axis; only the upper one is stable in the vertical direction. Increasing the current further, one successively goes through various MG potential well configurations around the successive stable levitation points. The well shapes are, respectively, prolate ellipsoids (between V and S), spheres (point S), oblate ellipsoids (between S and H), and horizontal planes (point H). The example here is for LH2, but the same is true of other liquids, such as water [8]. For a single solenoid, the residual forces around the stable compensation point can only be modified if the position of this point is changed and consequently the current too. Practically, there can be a technological limitation due to the maximal current value, resulting from the cooling of resistive magnets, or the critical surface of superconducting magnets. Since the spherical harmonic coefficients of the magnetic field and so the field \mathbf{B} at any point in the working zone are uniquely related to the spatial derivatives of \mathbf{B} along the axis, for a single solenoid as well as for any axisymmetric set of windings, the above analysis can be applied if \mathbf{B} along the symmetry axis is known.

8.3.2 Improvement of Axisymmetric Device Performance

8.3.2.1 Ferromagnetic inserts

Magnetic force field distributions and thus MGE configurations can be changed by means of ferromagnetic inserts located close to the working zone. Figure 8.3 shows a ring-shaped insert that could be used to enlarge the 1 % inhomogeneity levitation zone (equivalent insert has been manufactured at CEA Grenoble, HyLDe facility). Elongation of the ellipsoidal MG well was obtained, using this insert. If the ferromagnetic insert becomes saturated, the norm of \mathbf{G} (hence the magnetic force magnitude) is no longer proportional to the square of the solenoid current.

8.3.2.2 Multiple solenoid devices and special windings design

As of 1999, multiple solenoid devices were designed to increase field, magnetic forces, and improve magnetic compensation quality [9, 10], but without MGE tuning. A control of the different currents in multiple coil levitation devices should allow for continuous tuning of the MGE around perfect levitation points. As far as we know, the best device for MGE tuning should be a set of harmonic coils where each coil would be fed by independent current.

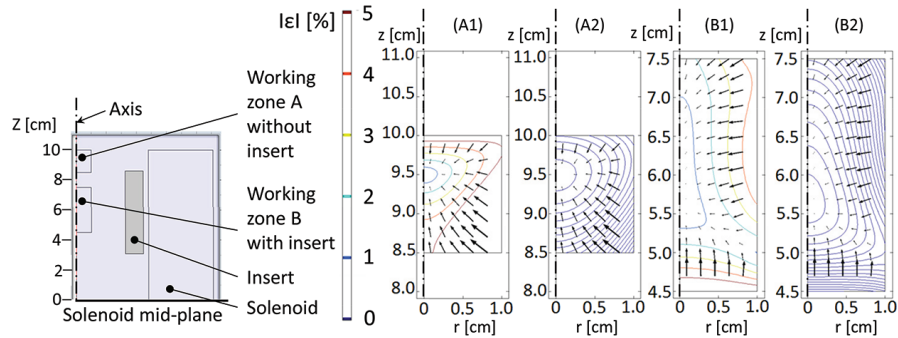


Figure 8.3 Comparison of magnetic compensation quality within the bore of a single solenoid with and without insert. On the *left* is an overview of the system. Adding an insert modifies the force configuration. The levitation points are changed as well as the current needed to reach the levitation. Thus, there are two different working zones: **A** (no insert, $J_A = 218.28 \text{ A mm}^{-2}$) and **B** (insert, $J_B = 251.94 \text{ A mm}^{-2}$). Working zone location and current are defined so as to get the largest levitated volume at given homogeneity. The resulting acceleration (*black arrows*) shows that levitation is stable inside both of the cells **A** and **B**. Isohomogeneity (*color curves*) is provided from 1 to 5 % by step of 1 % in figures **A1** and **B1**. MGE iso- Σ_L (*blue curves*) are elongated by the insert in the vertical direction as shown in figure **B2** w.r.t. figure **A2**.

This multicoil device allowing arbitrary control of the first three harmonics would enable quick variation of gravity by rapid current variation in one coil, as well as easy adjustment of residual forces [11]. Such a design has not been built yet. This approach leads to device design dedicated to the creation of useful magnetic force distributions for specific applications. For example, an axisymmetric distribution of \mathbf{B} varying as $B_0 (z - z_0)^{1/2}$ on the vertical axis of symmetry, generated by an appropriate current distribution in the windings, gives a constant norm of \mathbf{G} along a vertical segment (but not in a whole 2D axisymmetric domain); here, B_0 and z_0 are constants. Besides axisymmetric coils, the development of saddle coils for particle accelerator magnets should allow for new types of levitators with a long working zone. The general theory for axisymmetric systems can be easily transposed to these magnets. It is worth noticing that the theoretical development presented here can be applied to permanent magnet systems. High-coercivity magnets are in any way equivalent to high value of surface current density (A m^{-1}), leading to high magnitude of \mathbf{G} in narrow zones, near magnet edges. Such permanent magnet systems have been designed for free-contact handling of diamagnetic microdroplets (biomedical applications). Levitation is observed if the integrated magnetic volume force over the whole droplet volume counterbalances the droplet weight since the surface tension is very high at those dimensions (levitation similar to that of a rigid body); therefore, the quality of local compensation is not an issue.

8.4 Magnetic Gravity Compensation in Fluids

Many experiments in magnetic gravity compensation focus on fluid mechanics, especially on gas bubbles, liquid drops, and diphasic fluids with or without temperature gradient [3, 8, 12–18]. An important issue when levitating a drop or bubble is the stability of mechanical equilibrium. Drops and bubbles are stable when they are trapped within a well of the MG potential. Stable diamagnetic levitation of droplets inside a vertical-axis single solenoid is possible in the upper region of the solenoid (marked “+” on Figure 8.1). Conversely, paramagnetic levitation of bubbles occurs in the lower part of the solenoid, and only the lowest levitation point is stable in the vertical direction. In stable mechanical equilibrium, the center of a vanishingly small and spherical bubble, or droplet, is located at the local minimum of the MG potential Σ_L . For finite-sized droplets or bubbles, both its shape and its equilibrium position depend on various parameters: surface tension of the liquid/gas interface, the MG potential well shape, and demagnetization

energy. The latter is due to the magnetic field modification because the gas/liquid interface shape always tends to elongate paramagnetic bubbles or diamagnetic droplets in the magnetic field direction. This effect has been revealed [13] and then analyzed [14] in paramagnetic liquid oxygen. For a diamagnetic gas/liquid interface, this effect can be neglected due to the weakness of the magnetic susceptibility. Interface shape is then given by equilibrium of surface tension and MG potential [8, 15]. When diamagnetic liquids are close enough to their critical point, the interface shape tends to that of the MGE [18]. In paramagnetic fluids, patterning effects of the liquid/gas interface may be observed when the magnetic field is perpendicular to the interface [19]. This effect, well known for ferrofluids, can make levitation useless in paramagnetic diphasic systems such as liquid/gas oxygen. Thermal exchanges have been studied in various boiling regimes [13]. Observed phenomena, bubble size and growth rate, are far different from those under normal gravity but rather similar to what happens in real weightlessness. Magneto-convection can appear in paramagnetic monophasic fluid due to the susceptibility dependency on the temperature. This effect has been observed and investigated by means of a magnetic Rayleigh number [20]. All of these examples of bubble shape stability, gas/liquid interface modifications, and thermal convection demonstrate that the microgravity environment generated by magnetic field can, in many ways, closely mimic true weightlessness. However, the strong magnetic field can produce other effects not observed in weightlessness. Some of these effects can be mitigated by magnet design, through the harmonic contents of the field.

8.5 Magnetic Gravity Compensation in Biology

Since Geim and coworkers [2] demonstrated levitation of a live frog and Valles et al. [4] studied a levitating frog's egg in 1997, diamagnetic levitation has been used in experiments on a variety of biological organisms, including, for example, *Paramecia* [21], yeast [22, 23], *Arabidopsis* plants [23–25] and cell cultures [26–28], bacteria [29–31], bone cells [32–36], a live mouse [37], and fruit flies [38, 39].

Since the diamagnetic force is a body force, like the gravitational force, we can write the net force acting on the object in the magnetic field in terms of an *effective* gravitational field, $\Gamma = g\varepsilon = \mathbf{g} + (\chi/\rho)\mathbf{G}/(2\mu_0)$; ε , \mathbf{g} , and \mathbf{G} are as defined above. The ratio χ/ρ is constant for a homogeneous substance such as water or a well-mixed solution. Spatial variations in Γ owing to spatial variation of the magnetic field exert weak tidal forces on an object in

the magnetic field: variation in Γ is typically $\sim 0.5 \text{ m s}^{-2}$ per cm in current experiments [8], but can be made as small as one like along a line segment using a suitable solenoid design [40].

For biological material, χ/ρ cannot be taken as a constant: It varies depending on the tissue type. For most soft biological tissues, $-11.0 \times 10^{-6} < \chi < -7.0 \times 10^{-6}$ [41], close to the value for water, -9×10^{-6} . Iron-rich tissues have slightly more positive susceptibility owing to the paramagnetism of the Fe ion. However, even an iron-rich organ such as liver has susceptibility only slightly more positive than water. Table 8.2 gives the susceptibilities of a few biological materials, along with approximate densities ρ . Variations in χ/ρ between different material types give rise to variations in the effective gravity Γ throughout the organism, generating physical stresses akin to the above-mentioned tidal forces. Values of $\varepsilon = \Gamma/g$ at the stable levitation point of water are given in the table, to enable comparison. At the levitation point of the *organism*, determined by its mean susceptibility (usually close to that of water) and density, the magnitude of Γ may be slightly smaller: Experiments on freely levitating frogs' eggs determined the magnitude of Γ acting on three main constituents of the egg fractionated by centrifugation—the cytosol, a protein-rich pellet, and lipids—to be 0.02 g, 0.075 g, and 0.06 g, respectively [4].

Table 8.2 suggests that relatively dense materials, such as bone and starch, will experience a significant fraction of g even in a freely levitating organism. Substantiating this, experiments show that a growing plant root can readily establish the direction of real gravity when levitating [23, 25], consistent with the theory that plants use the position of starch-rich *statoliths* within the cells at the root tip to sense which way is down. The buoyancy of a

Table 8.2 Volume susceptibility χ and approximate density ρ of some biological materials and tissues, including the magnitude of the effective gravity $\varepsilon = |\Gamma|/g$ and its direction (up or down with respect to gravity, indicated by arrows), calculated at the levitation point of water

	χ (10^{-6})	ρ (kg m^{-3})	ε (at lev. pt. water)
Water (37 °C)	-9.05 [41]	993 [41]	0
Cytosol of a frog's egg	-9.09 [4]	1,030 [4]	0.03↓
Stearic acid (20 °C)	-10.0 [41]	940 [42]	0.18↑
Starch	-10.1 [43]	1,530 [42]	0.27↓
Whole blood, human (deoxyg.)	-7.90 [41]	1,040 [44]	0.16↓
Liver, human (healthy)	-8.8 [41]	1,050 [41]	0.08↓
Cortical bone, human	-8.9 [41]	1,900 [44]	0.49↓
Cholesterol	-7.61 [45]	1,020 [45]	0.18↓

statolith within a root cell is altered by the field gradient \mathbf{G} , through the magneto-Archimedes effect [19, 46]. The magnitude of \mathbf{G} required to keep a statolith *neutrally buoyant* within the cell is 3–4 times as large as that required to levitate water [23]. Such differences in \mathbf{G} required for flotation can also be exploited for separation of biological [45] and non-biological materials [19]. Magneto-Archimedes buoyancy can also be responsible for magneto-convection in liquid microbiological cultures [30].

In order to differentiate between effects of levitation and any other effects of the strong magnetic field, at least two chambers containing the biological samples are usually placed in the magnetic field, one enclosing the point where the sample levitates and another enclosing the geometric center of the solenoid, where $\mathbf{G} = \mathbf{0}$. The central chamber is used to control for other effects of magnetic field, besides levitation. Chambers may be placed at other points in the field to simulate Martian or lunar gravity for example [5], or to simulate hypergravity. The confinement of the chamber may be used to restrict the range of effective gravities to which the organism is exposed and is made as small as required for this purpose. Comparing levitating samples with those in 2 g hypergravity can reveal the relative influence of stresses induced by differences between Γ acting on different tissue types; if such stresses dominate, results from levitation and 2 g would be expected to be similar [39]. Using this technique, the movements of levitating fruit flies were found to be consistent with those observed in true weightlessness, with no other effects of the strong magnetic field observed [39]. In other experiments, effects of the strong field (~ 10 T) are observed, besides that of levitation; see, for example, Refs. [31, 38, 47, 48].

The evidence emerging from experiments on a variety of different organisms suggests that levitation can compensate gravity quite effectively. In studies on frogs' eggs, for example, the authors find [4], "the reduction in body forces and gravitational stresses achieved with magnetic field gradient levitation. . . has not been matched by any other ground-based, low-gravity simulation technique." One should be aware, however, of the variation in effective gravity between different tissue types, particularly for higher-density materials such as bone, and that the strong magnetic field may influence the organism through other mechanisms, which may mask the effect of altered gravity.

Acknowledgments

We would like to thank the SBT-CEA-Grenoble for data about HyLDe facility.

References

- [1] Beaugnon, E. and R. Tournier. “Levitation of Organic Materials.” *Nature* 349(1991): 470.
- [2] Berry, M.V. and A.K. Geim. “Of Flying Frogs and Levitrons.” *European Journal of Physics*. 18 (1997): 307–313.
- [3] Weilert, M.A., D.L. Whitaker, H.J. Maris and G.M. Seidel. “Magnetic Levitation and Noncoalescence of Liquid Helium.” *Physical Review Letters*. 77 (1996): 4840 and “Magnetic Levitation of Liquid Helium.” *Journal of Low Temperature Physics*, 106 (1997): 101–131.
- [4] Valles, J.M., Jr., J.M. Denegre and K.L. Mowry. “Stable Magnetic Field Gradient Levitation of *Xenopus laevis*: Toward Low-Gravity Simulation.” *Biophysical Journal* 731130-1133 (1997): 1130–1133.
- [5] Valles, J.M., Jr., H.J. Maris, G.M. Seidel, J. Tang and W. Yao. “Magnetic Levitation-Based Martian and Lunar Gravity Simulator”. *Advances in Space Research* 36 (2005): 114–118.
- [6] Quettier, L., et al. “Magnetic Compensation of Gravity in Liquid/Gas Mixtures: Surpassing Intrinsic Limitations of a Superconducting Magnet by Using Ferromagnetic Inserts.” *European Physical Journal Applied Physics* 32, no. 3 (2005): 167–175.
- [7] Lorin, C. and A. Mailfert. “Magnetic Compensation of Gravity and Centrifugal Forces.” *Microgravity Science and Technology* 21 (2009): 123–127.
- [8] Hill, R.J.A. and L. Eaves. “Vibrations of a Diamagnetically Levitated Water Droplet.” *Physical Review E* 81(2010): 056312; *ibid.* 85 (2012): 017301.
- [9] Bird, M.D. and Y.M. Eyssa. “Special Purpose High Field Resistive Magnets.” *IEEE Transactions on Applied Superconductivity* 10 (2000): 451–454.
- [10] Ozaki, O., et al.. “Design Study of Superconducting Magnets for Uniform and High Magnetic Force Field Generation.” *IEEE Transactions on Applied Superconductivity* 11 (2001): 2252–2255.
- [11] Lorin, C. and A. Mailfert. “Design of a Large Oxygen Magnetic Levitation Facility.” *Microgravity Science and Technology* 22 (2010): 71–77.
- [12] Nikolayev, V., D. Chatain, D. Beysens and G. Pichavant. “Magnetic Gravity Compensation.” *Microgravity Science and Technology* 23(2011): 113–122.

- [13] Pichavant, G., B. Cariteau, D. Chatain, V. Nikolayev and D. Beyens. “Magnetic Compensation of Gravity: Experiments with Oxygen.” *Microgravity Science and Technology* 21 (2009): 129–133.
- [14] Duplat, J. and A. Mailfert. “On the Bubble Shape in a Magnetically Compensated Gravity Environment.” *Journal of Fluid Mechanics* 716 (2013): R11.
- [15] Chatain, D. and V. Nikolayev. “Using Magnetic Levitation to Produce Cryogenic Targets for Inertial Fusion Energy: Experiment and Theory.” *Cryogenics* 42 (2002): 253–261.
- [16] Beaugnon, E., D. Fabregue, D. Billy, J. Nappa and R. Tournier. “Dynamics of Magnetically Levitated Droplets.” *Physica B* 294–295 (2001): 715–720.
- [17] Hill, R.J.A. and L. Eaves. “Nonaxisymmetric Shapes of a Magnetically Levitated and Spinning Water Droplet.” *Physical Review Letters* 101 (2008): 234501.
- [18] Lorin, C., et al. “Magnetogravitational Potential Revealed Near a Liquid–Vapor Critical Point.” *Journal of Applied Physics* 106 (2009): 033905.
- [19] Catherall, A.T., L. Eaves, P.J. King and S.R. Booth. “Floating Gold in Cryogenic Oxygen.” *Nature* 422 (2003): 579.
- [20] Braithwaite, D., E. Beaugnon and R. Tournier. “Magnetically Controlled Convection in a Paramagnetic Fluid.” *Nature* 354 (1991): 134–136.
- [21] Guevorkian, K. and J.M. Valles, Jr. “Swimming *Paramecium* in Magnetically Simulated Enhanced, Reduced, and Inverted Gravity Environments.” *Proceedings of the National Academy of Sciences of the United States of America* 35 (2006): 13051–13056.
- [22] Coleman, C.B., et al. “Diamagnetic Levitation Changes Growth, Cell Cycle, and Gene Expression of *Saccharomyces cerevisiae*.” *Biotechnology and Bioengineering* 98 (2007): 854–863.
- [23] Larkin, O.J. “Diamagnetic Levitation: Exploring the Effects of Weightlessness on Living Organisms.” Ph.D. Thesis, University of Nottingham (2010).
- [24] Brooks J.S., et al. “New Opportunities in Science, Materials, and Biological Systems in the Low-Gravity (magnetic levitation) Environment (invited).” *Journal of Applied Physics* 87 (2000): 6194–6199.
- [25] Herranz, R., et al. “Ground-Based Facilities for Simulation of Microgravity: Organism-Specific Recommendations for their Use, and Recommended Terminology.” *Astrobiology* 13 (2012): 1–17.
- [26] Babbick, M., et al. “Expression of Transcription Factors After Short-Term Exposure of *Arabidopsis thaliana* Cell Cultures to Hypergravity

- and Simulated Microgravity (2-D/3-D Clinorotation, Magnetic Levitation).” *Advances in Space Research* 39 (2007): 1182–1189.
- [27] Manzano, A.I., et al. “Gravitational and Magnetic Field Variations Synergize to Cause Subtle Variations in the Global Transcriptional State of *Arabidopsis* In Vitro Callus Cultures.” *BMC Genomics* 13 (2012): 105.
- [28] Herranz, R., A.I. Manzano, J.J.W.A van Loon, P.C.M. Christianen and F.J. Medina. “Proteomic Signature of *Arabidopsis* Cell Cultures Exposed to Magnetically Induced Hyper- and Microgravity Environments.” *Astrobiology* (2013). doi:10.1089/ast.2012.0883 (online before print).
- [29] Beuls, E., R. Van Houdt, N. Leys, C.E. Dijkstra, O.J. Larkin and J. Mahillon. “*Bacillus thuringiensis* Conjugation in Simulated Microgravity.” *Astrobiology* 9 (2009): 797–805.
- [30] Dijkstra, C.E., et al. “Diamagnetic Levitation Enhances Growth of Liquid Bacterial Cultures by Increasing Oxygen Availability.” *Journal of the Royal Society Interface* 6 (2011): 334–344.
- [31] Liu, M., et al. “Magnetic Field is the Dominant Factor to Induce the Response of *Streptomyces avermitilis* in Altered Gravity Simulated by Diamagnetic Levitation.” *PLoS One* 6 (2011): e24697.
- [32] Hammer, B.E., L.S. Kidder, P.C. Williams and W.W. Xu. “Magnetic Levitation of MC3T3 Osteoblast Cells as a Ground-Based Simulation of Microgravity”. *Microgravity Science and Technology* 21(2009): 311–318.
- [33] Qian, A., et al. “cDNA Microarray Reveals the Alterations of Cytoskeleton-Related Genes in Osteoblast Under High Magneto-Gravitational Environment.” *Acta Biochimica et Biophysica Sinica (Shanghai)* 41 (2009): 561–577.
- [34] Qian, A.R., et al. “High Magnetic Gradient Environment Causes Alterations of Cytoskeleton and Cytoskeleton-Associated Genes in Human Osteoblasts Cultured In Vitro.” *Advances in Space Research* 46 (2010): 687–700.
- [35] Wang, L., et al. “Diamagnetic Levitation Causes Changes in the Morphology, Cytoskeleton, and Focal Adhesion Proteins Expression in Osteocytes.” *IEEE Transactions on Biomedical Engineering* 59 (2012): 68–77.
- [36] Qian, A.-R., et al. “Large Gradient High Magnetic Fields Affect Osteoblast Ultrastructure and Function by Disrupting Collagen I or Fibronectin/ $\alpha\beta$ 1 Integrin.” *PLoS One* 8e51036 (2013): e51036.

- [37] Liu, Y., D.-M. Zhu, D. M. Strayer and U.E. Israelsson. “Magnetic Levitation of Large Water Droplets and Mice.” *Advances in Space Research* 45 (2010): 208–213.
- [38] Herranz, R., et al. “Microgravity Simulation by Diamagnetic Levitation: Effects of a Strong Gradient Magnetic Field on the Transcriptional Profile of *Drosophila melanogaster*.” *BMC Genomics* 13 (2012): 52.
- [39] Hill, R.J.A., et al. “Effect of Magnetically Simulated Zero-Gravity and Enhanced Gravity on the Walk of the Common Fruit Fly.” *Journal of the Royal Society Interface* 9 (2012): 1438–1449.
- [40] Lorin, C., A. Mailfert, C. Jeandey and P.J. Masson. “Perfect Magnetic Compensation of Gravity Along a Vertical Axis.” *Journal of Applied Physics* 113 (2013).
- [41] Schenck, J.F. “The Role of Magnetic Susceptibility in Magnetic Resonance Imaging: MRI Magnetic Compatibility of the First and Second Kinds.” *Medical Physics* 23 (1996): 815–850 (and references therein).
- [42] Haynes, W.M. (ed.), *Handbook of Chemistry and Physics. 93rd edition*. Boca Raton, FL, CRC Press, 2012.
- [43] Kuznetsov, O.A. and K.H. Hasenstein. “Intracellular Magnetophoresis of Amyloplasts and Induction of Root Curvature.” *Planta* 198 (1996): 87–94.
- [44] Cameron, J.R., J.G. Skofronick and R.M. Grant. “Physics of the Body”. Madison WI, Medical Physics Publishing, 1992.
- [45] Hirota, N., et al. “Magneto-Archimedes Separation and its Application to the Separation of Biological Materials.” *Physica B* 346-347 (2004): 267–271.
- [46] Ikezoe, Y., et al. “Making Water Levitate,.” *Nature* 393 (1998): 749.
- [47] Denegre, J.M., J.M. Valles Jr., K. Lin, W.B. Jordan and K.L. Mowry. “Cleavage Planes in Frog Eggs are Altered by Strong Magnetic Fields.” *Proceedings of the National Academy of Sciences of the United States of America* 95 (1998): 14729–14732.
- [48] Iwasaka, M., J. Miyakoshi and S. Ueno. “Magnetic Field Effects on Assembly Pattern of Smooth Muscle Cells.” *In Vitro Cellular & Developmental Biology—Animal* 39 (2003): 120–123.

